The University of Wisconsin Library
Manuscript Theses

This thesis by RIMANTAS P. BUINEVICIUS
has been used by the following persons, whose signatures attest their acceptance of the above restrictions.

A Library which borrows this thesis for use by its patrons is expected to secure the signature of each user.

NAME AND ADDRESS	DATE

F-4244

A THREE-WAVELENGTH PULSE OXIMETER
FOR CARBOXYHEMOGLOBIN DETERMINATION

by

RIMANTAS P. BUINEVICIUS

A thesis submitted in partial fulfillment of the
requirements for the degree of

MASTER OF SCIENCE
(Electrical and Computer Engineering)

at the
UNIVERSITY OF WISCONSIN-MADISON
1987

Abstract

Pulse oximetry measures the relative concentration of arterial oxygenated hemoglobin and reduced hemoglobin. This paper presents the design of a pulse oximeter which measures the presence of a third substance, carboxyhemoglobin (HbCO), by unfiltered LEDs at 660 nm, 810 nm, and 940 nm. It presents theoretical approximations and calculations which are implemented in our instrument. It includes sensor design and a flowchart, which shows the signal processing routine that accomplishes the required analysis.

Introduction

Oximeters. The first oximeters used spectrophotometry at two wavelengths on withdrawn blood. Upon withdrawal, the blood sample is placed in a cuvette and exposed to two or more monochromatic beams of light. The transmitted light is detected by a photocell whereupon the signal is amplified and put through calculations to estimate the saturation of hemoglobin. In order to avoid withdrawal of blood, this technique was extended by using fiber optics to transmit the wavelengths into and back from the blood [1]. This technique can measure $\%O_2$ saturation (SaO_2) noninvasively by transmitting light through the pinna of the ear or by reflecting light from the finger pad.

Pulse oximeters. A new method, different from the above is pulse oximetry. It relies on the arterial pulsations of a given appendage. The change in light transmission due to the arterial inflow corresponds to the same transmission as the spectrophotometric case except that the dc level of light transmission must be eliminated. The dc portion is made up of nonchanging entities such as tissue, venous blood, bone, etc. [2]. Pulse oximetry provides a noninvasive method of determining arterial oxygen saturation.

Three-component oximeters. Oximeters have distinguished only two components: hemoglobin and oxygenated hemoglobin. The ability to measure a third component, carboxyhemoglobin, can offer a useful addition. Also, present systems yield inaccurate results when substantial amounts of carbon monoxide are bound to blood [3]. Clinical testing has shown that most oximeters suffer from nonlinearity below 70% SaO_2 and that carboxyhemoglobin, methemoglobin, and sulfhemoglobin are the cause of some of these errors [4].

Reflectance oximeters. It would be desirable to show that a skin reflectance pulse oximeter capable of monitoring three components has the potential of displacing transmission oximeters. Reflectance oximeters are more complex because they increase the scattering of light [5],[6],[7],[8]. Reflectance oximeters have not gained wide popularity in pulse oximetry because the sensor and emitter are on the same side of the finger, which increases scattering. Depending on the appendage size, the scattering causes greater or lesser amounts of light to be transmitted to the sensor such that the light may even saturate the output amplifier connected to the sensor. At best this causes large variations in base dc levels if the emitter beam is not sharply focussed. However, both transmission and reflectance oximeters share LED technologies and absorption coefficient data. The absorption coefficients used by both techniques differ only because of each instrument's inherent geometry and circuit components. The source of light (nonfocussed LEDs), the angle of light emission, and the intensity all play large roles in determining the absorption coefficients. Data for monochromatic light have been reported throughout the literature. It would be desirable to achieve standard absorption coefficients for the broader bandwidth LEDs as light sources.

This paper presents a system to measure three components of hemoglobin bonding based on the presence of one of those components, carbon monoxide. It presents theoretical curves which simulate the anticipated results and the resulting calculations. Techniques are presented which help simplify the calculation procedure. An outline of the oximeter's hardware, software, and sensor are covered. Further, the system provides further information on using broad spectrum LEDs and how to obtain correct absorption coefficients using them.

Oximeter Theory

Beer's law. Traditional oximeters have solved Beer's law for two components: oxygenated hemoglobin (HbO_2) and reduced hemoglobin (Hb). Beer's law is:

$I = I_0 \, 10^{-ecd}$ (1)

where I = transmitted light, I_0 = incident light, e = absorption coefficient of the substance at some wavelength, c = concentration of the absorbing substance, and d = optical path length through the substance. Transmission T is related to absorption A by: $A = -\log T$ (2)

where

$T = I/I_0$ (3)

thus yielding

$A = -\log ecd$ (4)

Equation (4) can be expanded to include the effects of multiple absorbing materials.

$A = e_1c_1d + e_2c_2d + e_3c_3d \ldots$ (5)

We substitute the absorption coefficients for three substances and measure the absorbance at three wavelengths to obtain three equations:

$A_1 = e_{11}c_1d + e_{12}c_2d + e_{13}c_3d$ (6)

$A_2 = e_{21}c_1d + e_{22}c_2d + e_{23}c_3d$ (7)

$A_3 = e_{31}c_1d + e_{32}c_2d + e_{33}c_3d$ (8)

If we assume that only three components exist, namely Hb, HbO_2, and HbCO, we can make the following substitutions: A_1, A_2, and A_3 correspond to the absorbances at 660 nm, 805 nm, and 940 nm, respectively, which were chosen due to the commercial availability of LEDs at these wavelengths and their fairly wide spectral separation from each other;c_1, c_2, and c_3 correspond to the concentrations of Hb, HbO_2, and HbCO, respectively; e_{11}, e_{21}, and e_{31} correspond to the absorption coefficients of Hb at 660 nm, 805 nm, and 940 nm, respectively; e_{12}, e_{22}, e_{32} correspond to the absorption coefficients of HbO_2; and e_{13}, e_{23}, and e_{33} correspond to the absorption coefficients of HbCO.

Dividing (6) by (7) and (8) by (6) we can eliminate the distance component d. Note that the arterial inflow of blood can cause a time dependent variation of d, even though this value would prove to be slight. Nevertheless, whether d remains constant, assuming rigidity of the finger artery, or varies to a certain extent, its variability can be eliminated by dividing the elements of equation (6) by (7):

$$\frac{A_1}{A_2} = \frac{e_{11}c_1 + e_{12}c_2 + e_{13}c_3}{e_{21}c_1 + e_{22}c_2 + e_{23}c_3} \quad (9)$$

and (8) by (6):

$$\frac{A_3}{A_1} = \frac{e_{31}c_1 + e_{32}c_2 + e_{33}c_3}{e_{11}c_1 + e_{12}c_2 + e_{13}c_3} \quad (10)$$

We also assume that only three products are attached to hemoglobin (Hb, HbO_2, HbCO) and that these make up 100% of the hematocrit, thus a third equation is $c_1 + c_2 + c_3 =$ 100%, where c_1, c_2, and c_3 are expressed as percentages.

For case 1, where we calculate A_{660}/A_{805} we can substitute the value of c_1 with $c_1 = 100 - c_2 - c_3$. At 805 nm $e_{21} = e_{12}$, thus

$$\frac{A_{660}}{A_{805}} = \frac{100e_{11} + c_2(e_{12} - e_{11}) + c_3(e_{13} - e_{11})}{100e_{21} + c_3(e_{23} - e_{21})} \quad (11)$$

This reduces to a set of linear equations where the slope and the intercept are functions of c_3.

$$m_1 = \frac{e_{12} - e_{11}}{100e_{21} + c_3(e_{23} - e_{21})} \quad (12)$$

and

$$Y_1 = \frac{c_3(e_{13} - e_{11}) + 100e_{11}}{100e_{21} + c_3(e_{23} - e_{21})} \quad (13)$$

A similar formulation can be made for A_{940}/A_{660}, however the slope and intercept, will vary as a function of c_2, the x value of the equation.

$$m_2 = \frac{(e_{32} - e_{31})}{100e_{11} + c_2(e_{12} - e_{11}) + c_3(e_{13} - e_{11})} \quad (14)$$

$$Y_2 = \frac{100e_{31} + c_3\ (e_{33} - e_{31})}{100e_{11} + c_2(e_{12} - e_{11}) + c3(e_{13} - e_{11})} \quad (15)$$

<u>Pulse Oximetry</u>. Pulse oximetry assumes that the

pulsatile arterial inflow causes a modulation in transmittance [2],[9]. If the sensor measures a dc level (E_{dc}) during diastole, arterial pulsations cause an increased attenuation in the amount of light that is transmitted during systole. This variation can be termed the ac response (E_{ac}). The dc level is entirely due to nonchanging entities such as venous blood, tissue, bone, skin, etc. Transmittance is given by:

$$T = \frac{E_{dc} + E_{ac}}{E_{dc}} \qquad (16)$$

By taking the log of T, we obtain the absorbance A and can then substitute into (6), (7), and (8).

Absorbance Ratios

Figure 1 shows a 3-D representation of the two different ratios of absorbances plotted on the x and y axes versus the hemoglobin saturation on the z axis. Isolateral lines represent variation of HbCO. Thus all five varying factors are plotted on one graph. The surface therefore represents the complete solution to Beer's law with our three components, but presents difficulty in estimating the actual saturation since there may be multiple solutions to concurrent ratios.

The 2-D graphs of Fig. 2, Fig. 3, and Fig. 4 are more informative. The A_{660}/A_{805} ratio and A_{940}/A_{660} yield two very different plots. The A_{660}/A_{805} ratio yields a linear plot whereas the A_{940}/A_{660} yields a plot with varying intercept and slope as predicted by (14) and (15). This is due to the isosbestic point (where the absorbances are equal) in ratio 1 versus the lack of one in ratio 2. From the measured absorbance ratio in Fig. 2, we draw a horizontal line through all solutions, and then do the same for the second ratio in Fig. 3. We then overlay Fig. 2 onto Fig. 3 as shown in Fig. 5. Running vertical lines we can find the two points which match up with the same percentage of HbCO and HbO_2. This corresponds to our unique solution to the equations.

Oximeter Calibration

Absorption Coefficients. It would be easiest to use monochromatic sources of light to calibrate an oximeter. We could simply use published results of the absorption coefficient for the wavelengths being used. Any changes due to components and geometry could be made by simply scaling all the values by the same factor or making small changes in individual coefficients. For low cost and compact size, we use LEDs which are not monochromatic, but have a small to medium bandwidth.

Incorporating individual LEDs creates some problems, but these can be overcome. The use of nonfiltered LEDs has been reported previously [10] where it was stressed that the difference between absorption coefficients for oxygenated and deoxygenated hemoglobin was of great importance. However, we have found that the concentration of reduced hemoglobin and carboxyhemoglobin both make up the deoxyhemoglobin and that both have considerably different spectral characteristics. Thus, the absorption coefficients for both substances must be established along with the base value for oxygenated hemoglobin. At 940 nm and 805 nm, carboxyhemoglobin has a much lower absorption coefficient than reduced hemoglobin and therefore using the equations for two components causes large error when HbCO contamination is present.

Clinical procedure. Finding the absorption coefficients required clinical verification and actual drawn samples. The absorption coefficient values were preset to values found in the literature on oximetry [10-13] although values tend to vary for each article. A sample of blood was then drawn. Its blood gas concentration was analyzed by an ICL 282 oximeter. The values recorded from the ICL 282 were compared to displayed results on our own oximeter. By knowing the actual concentrations of Hb, HbO_2, and HbCO and also the different absorbance ratios, it was possible to solve for the absorption coefficients by plugging the known components into equations 9 and 10. The first blood sample was fully oxygenated. The patient breathed pure O_2 and blood was drawn by arterial puncture. This yielded ratios for e_{12}, e_{22}, and e_{32}. Since the absorption coefficient of Hb at 805 nm is near e_{22} then $e_{22} = e_{21}$. The absorption coefficient at 650 nm for O_2 and CO is similar so that $e_{12} = e_{13}$. Four coefficients remain to be determined: e_{11}, e_{23}, e_{31}, e_{33}. These are reduced hemoglobin at 660 nm and 940 nm and carboxyhemoglobin at 805 nm and 940 nm.

The patient was allowed to breath a lung diffusion mixture containing 0.4% CO balance air. After 100 breaths the HbCO level of the subject had increased to approximately 15-17% HbCO. The strong binding of CO proved useful because very little Hb remained. Thus the ratios depended on only two components HbO_2 and HbCO. We used the absorption coefficient approximation of HbCO at 660 nm as a starting point. It was a simple matter of finding the necessary coefficient at 940 nm to make the ratio found equal to the theoretical ratio. Likewise at 805 nm, the ratio was easily used to find the absorption coefficients of HbCO at 805 nm. The absorption coefficient of HbCO at 805 nm and 940 nm is small and contributes little to the overall ratio. Thus it must be known accurately to avoid errors in the two absorption ratios. The widely changing characteristics of the absorption coefficients and the difficulties of line-fitting techniques suggested the use of matrix solutions to solve the set of simultaneous equations. Other techniques for solving the equations are given in the Appendix.

The best computational technique involves solving a 3 x 3 determinant since this guarantees that all points are at their correct isosbestic points. The solution of a 3 x 3 determinant requires obtaining the three absorbances at each wavelength. Subsequently, using the different absorbances and plugging them into [10] and [11] results in two ratios, A_{940}/A_{660} and A_{660}/A_{805}. Solving the first equation yields the unknowns of HbCO and HbO_2 and ratio 2 in Hb, HbO_2 and using a third equation 100% = HbO_2 + Hb + HbCO yields three equations in three unknowns. The use of A_{940}/A_{660} was purely by choice. A_{805}/A_{940} could have been used just as readily but creates a set of lines which do not show great separation (Fig. 4).

Oximeter Design.

Sensor. It was important to design the shape of the sensor to avoid transmission of stray light and entrance of ambient light. Ambient light entered the sensor and caused variability in dc output levels. Inclusion of a back panel blocked the ambient light and minimized this problem. Without finger pads, the nonfocussed LEDs permitted light to scatter around and from the finger to the sensor, saturating it and making it highly dependent on finger motion. Slight movement of the finger caused changes in the dc baseline setting of the sensor and errors in the results. Black silicone rubber pads which absorb the infrared as well as the red light minimized this problem. The pads contained 13 x 13 mm square holes which allowed some finger movement without causing much variation in displayed output. As long as the finger covered the square, little variation occurred. However, allowing light to pass upward and around the finger once again caused error.

Spring pressure proved to be a critical aspect of the sensor. The pressure exerted on the finger by a spring force of 0.5 N seemed to hold the sensor adequately without causing loss of circulation to the finger. Forces greater than 0.5 N caused discomfort and loss of pulse when applied for great lengths of time.

Besides the finger sensor, nose sensors and ear sensors are also used to measure oxygen saturation. These other sensors have the advantage of not being subjected to motion as are the finger sensors. The finger sensor can easily be implemented into an ear probe simply by changing the hardware assembly. A nose sensor would require a different design. Neither of these two sensors has yet been designed, but our system includes two connector control pins and software routines which will recognize the presence of these two other sensors.

Figure 6 shows that the emitter board, manufactured by Silicon Sensors, contains three custom-mounted LED dies arranged in a triangular formation and wire bonded while being mounted on gold inlay on epoxy resin board. The peak wavelengths of the LEDs are 660 nm, 810 nm, and 940 nm with bandwidths of 20 nm, 50 nm, and 50 nm, respectively. The LED dies are available from Silicon Sensors. The detector is a Siemens Corp. BPX-79 photovoltaic cell. Its rise time is 6 us and fall time is 10 us for 10% to 90% of minimal and maximal output. Maximal wavelength sensitivity is 800 nm. Sensitivity is 0.1 uA/lx minimum. The sensor assembly utilizes surface mount technology for its operational amplifier, resistors, and capacitors, all of which are mounted within the sensor compartment. Including the operational amplifier in the sensor assembly prevented interference problems from occurring within the 2.6 m length of nonshielded cable.

The LEDs are all rated between 10-20 mCd and provide more than adequate illumination at approximately 25 mA of current drain during normal operation. The on time is 100 us for each LED and the overall cycle time is 1/300 s. Figure 7 shows the circuit diagram for the sensor.

<u>Hardware</u>. The entire system is designed around a Hitachi 64180 CMOS microprocessor which is supported by a 64-kbyte EPROM and 2 kbyte of RAM. Information is

displayed on a customized LCD display. Data are retrieved via a 12-bit A/D converter which accepts the sensor output and digitizes it for input to the processor. The microprocessor controls the current driver. Each LED receives step inputs and self calibrates itself to a preset dc level (1.25 V) which is controlled via a feedback loop through the microprocessor. Each LED is connected to a separate output of the current driver and strobed in sequence after which a delay time occurs for energy conservation. Figure 8 shows the hardware layout.

<u>Software</u>. Software controls the LCD display, the current drivers, the data storage and the subsequent data analysis. The received data are integrated to stabilize the resulting values and eliminate erroneous data points. The software also has self checking routines for determining whether the finger is inserted, whether power is low, detection of a low pulse, etc. It also has built in safety features detecting the presence of low or high pulse, high levels of HbCO and low levels of HbO_2. An alarm sounds when any of these conditions are present. The sensor receives full software control through the current driver. Each LED is stepped in increments as a self test to indicate whether the sensor is working properly. The software also is capable of determining whether finger, ear, or nose sensor is connected to the unit. Figure 9

shows the flowchart of the software algorithm for calculating data.

Interfering substances

Under certain circumstances the percentage of methemoglobin and sulfhemoglobin would be substantial and cause error in our oximeter. Typically, the levels are relatively low and do not cause error for normal healthy individuals. However, patients taking drugs may have their iron oxidized from a ferrous form to a ferric form [14]. This methemoglobin is unable to take up oxygen and therefore has a different absorption spectrum. It may also occur under normal conditions in healthy individuals. Sulfhemoglobin conversion also occurs for certain drugs and causes irreversible inactive O_2 transport. Detection of both would be useful, but would greatly increase the complexity. Such detection is already possible through invasive optical techniques [4],[15].

Conclusion

We have presented the method and design of an instrument to measure the concentration of hemoglobin, oxygenated hemoglobin, and carboxyhemoglobin. Beer's law defines the three absorption equations at three separate wavelengths for nonfocussed LED sources. The plots of the three-dimensional and two-dimensional solutions to Beer's law help show an efficient way to calibrate an oximeter based on a unique set of absorption coefficients inherent to a given instrument. The graphing technique presented shows how to obtain unique solutions for different measured absorptions.

Observations made during this study showed it was necessary to add absorbing materials in the form of black plastic and black finger pads to eliminate scattering which caused fluctuating dc levels. Further, we noted that unusually high levels of sulfhemoglobin and methemoglobin may cause unsteady erroneous data to result.

Acknowledgement

I would like to thank Dr. John G. Webster for his technical support and guidance and also William N. Reining of Phoenix Engineering and Computing of Madison, WI who provided funding and coordination for this project.

APPENDIX

Solve module. There are two techniques which may approximate the relative percentage of the blood constituents. We have chosen to call them Kramer's solution and modified Kramer's solution [12].

Kramer's solution assumes a near isosbestic point at 660 nm. This point can be considered isosbestic due to the identical absorption coefficients of HbO_2 and HbCO, termed the mix component. The system is not capable of breaking up the two components. Therefore the assumption is made that they are one component at the ratio between 660 nm and 805 nm and would correspond to two components: i.e. that of Hb and the combination of HbO_2 and HbCO (Mix). Thus, we can extract the first percentage (Hb) relative to the total concentration using the ratio A_{660}/A_{805}. Following this procedure, it becomes necessary to perform the second calculation, that is breaking up the HbO_2 and HbCO to determine their relative concentrations in regards to the total concentrations. Thus a ratio of A_{940}/A_{660} would break apart the remaining two components and determine the concentration of HbO_2 and HbCO. Whether this technique works or not depends on the relative concentration of HbCO, since 805 nm is a wavelength where HbO_2 and HbCO have different coefficients. Further, the question arises as to how accurate such a system is if the concentration of HbCO is fairly high.

Substituting in equation 9 we have the case of e_{12} equal to e_{13} and e_{21} equal to e_{22}. This effectively separates Hb from Mix. Then solving the second ratio for HbCO and Mix we can obtain an error associated with Mix due to the presence of HbCO.

HbCO%	Mix%	
0	100	
10	99	
20	97	
30	95	... dizziness
40	93	
50	89	
60	85	... death
70	78	
80	67	
90	43	

This result indicates that as HbCO increases the Mix (HbCO + HbO2) declines. But the amount of decrease is relatively slow at first and the nonlinearity never equals the expected results. Further, as HbCO increases even more, it actually becomes greater than Mix. This is a direct result of assuming that the HbCO contribution at 805 nm is negligible.

The same error occurs for the A_{940}/A_{805} ratio where the Hb coefficient causes the nonlinearity. We can summarize the error produced by our instrument in the following table

-- Actual --			-- error --		
Hb%	HbO_2%	HbCO%	Hb%	HbO_2%	HbCO%
0	100	0	0.0	0.0	0.0
10	90	0	0.0	35.6	35.6
20	80	0	0.0	44.3	44.3
30	70	0	0.0	44.5	44.5
40	60	0	0.0	40.9	40.9
50	50	0	0.0	35.3	35.3
0	90	10	1.4	0.0	1.4
0	80	20	3.1	0.0	3.1
0	70	30	5.2	0.0	5.2
0	60	40	7.8	0.0	7.8
0	50	50	11.4	0.0	11.4
10	80	10	2.4	31.4	29.0
10	70	20	5.3	27.2	22.0
10	60	30	8.9	23.0	14.2
10	50	40	13.5	18.8	5.4
20	70	10	3.4	38.4	35.0
20	60	20	7.5	32.5	25.0
20	50	30	12.6	26.6	14.0
30	60	10	4.3	37.6	33.3
30	50	20	9.6	30.8	21.2
40	50	10	5.3	27.2	22.0

Note that the errors fluctuate greatly and that the only stable factor seems to be Hb.

For this reason we chose to implement a modified Kramer's solution to inspect the accuracy of a system which actually substitutes the value of HbO_2 + HbCO = Mix, whereas the regular Kramer solution assumed that Mix = HbO_2 at 805 nm. The solution to this implementation shows great correspondence in the 0-10% HbCO region, but falls off rapidly below HbCO equal to 10%.

-- ACTUAL --			-- ERROR FOR MODIFIED -- KRAMER'S SOLUTION		
Hb%	HbO_2%	HbCO%	Hb%	HbO_2%	HbCO%
0	100	0	0.0	0.0	0.0
10	90	0	0.0	0.0	0.0
20	80	0	0.0	0.0	0.0
30	70	0	0.0	0.0	0.0
40	60	0	0.0	0.0	0.0
50	50	0	0.0	0.0	0.0
0	90	10	1.4	8.4	9.8
0	80	20	3.1	16.5	19.6
0	70	30	5.2	24.1	29.3
0	60	40	7.8	31.0	38.9
0	50	50	11.4	36.9	48.3
10	80	10	2.4	7.4	9.8
10	70	20	5.3	14.3	19.6
10	60	30	8.9	20.4	29.3
10	50	40	13.5	25.4	38.9
20	70	10	3.4	6.4	9.8
20	60	20	7.5	12.1	19.6
20	50	30	12.6	16.7	29.3
30	60	10	4.3	5.5	9.8
30	50	20	9.6	9.9	19.6
40	50	10	5.3	4.5	9.8

REFERENCES

[1] R.A. Peura and J. G. Webster, "Basic transducers and principles," in Medical instrumentation application and design. Boston: Houghton Mifflin, 1978.

[2] I. Yoshiya, Y. Shimada, and K. Tanaka, "Spectrophotometric monitoring of arterial saturation in the fingertip", Med. Biol. Eng. Comput., vol. 18, pp. 27-32, 1980.

[3] K. P. Strohl, P. M. House, J. F. Holic, J. M. Fouke, and P. W. Cheung, "Comparison of three transmittance oximeters", Med. Instrum. vol. 20, pp. 143-149, 1986.

[4] A. Zwart, A. Buursma, B. Oeseburg and W. G. Zlijlstra, "Determination of hemoglobin derivatives with the IL 282 CO-oximeter as compared with a manual spectrophotometric five-wavelength method," Clin. Chem., vol. 27, pp. 1903- 1907, 1981.

[5] J. M. Steinke and A. P. Shepherd, "Role of light scattering in whole blood oximetry," IEEE Trans. Biomed. Eng., vol. BME-33, pp. 294-301, 1986.

[6] A. Cohen and N. Wadsworth, "A light emitting diode skin reflectance oximeter," Med. Biol. Eng., vol. 10, pp. 385-391, 1972.

[7] P. W. Cheung, S. Takatani and E. A. Ernst, "Multiple wavelength reflectance oximetry in peripheral tissues," Adv. Exp. Med. Biol., vol. 94, pp. 69-75,

1977.

[8] Y. Mendelson, P. W. Cheung, M. R. Neuman, D. G. Fleming and S. D. Cahn, "Spectrophotometric investigation of pulsatile blood flow for transcutaneous reflectance oximetry," Adv. Exp. Med. Biol., vol. 159, pp. 93-102, 1983.

[9] Y. Shimada, I. Yoshiya, N. Oka, and K. Hamaguri, "Effects of multiple scattering and peripheral circulation on arterial oxygen saturation measured with a pulse-type oximeter", Med. Biol. Eng. Comput., vol. 22, pp. 475-478, 1984.

[10] A. P. Shepherd, J. W. Kiel, and G. L. Riedel, "Evaluation of light emitting diodes for whole blood oximetry," IEEE Trans. Biomed. Eng., vol. BME-31, pp. 723-725, 1984.

[11] B. L. Horecker, "The absorption spectra of hemoglobin and its derivatives in the visible and near infra-red regions," J. Biol. Chem., vol. 143 B, pp. 173-183, 1943.

[12] K. Kramer, J. O. Elam, G. A. Saxton and W. N. Elam, "Influence of oxygen saturation, erythrocyte concentration and optical depth upon the red and near-infrared light transmittance of whole blood, Am. J. Physiol., vol. 165, pp. 229-246, 1951.

[13] E. Gordy and D. L. Drabkin, "Spectrophotometric

studies: XVI. Determination of the oxygen saturation of blood by a simplified technique, applicable to standard equipment," J. Biol. Chem., vol. 227, pp. 285-299, 1957.

[14] R. M. Berne and M. N. Levy, Physiology. St. Louis, MO: C.V. Mosby, 1983.

[15] H. O. Michel and J. S. Harris, "The properties and quantitative determination with special reference to the spectrophotometric methods," J. Lab. Clin. Med., vol. 25, pp. 445-463, 1940.

FIGURE LEGENDS

Figure 1. A three-dimensional representation of carboxyhemoglobin plotted as a function of the hemoglobin saturation and absorbance ratios at 940 nm/660 nm and 660 nm/805 nm.

Figure 2. The plot of absorbance at 660 nm/ absorbance at 805 nm versus the percentage of oxyhemoglobin (HbO_2). The different lines represent stepwise variations in carboxyhemoglobin (HbCO).

Figure 3. The plot of absorbance at 940 nm/ absorbance at 660 nm versus the percentage of oxyhemoglobin. The different lines represent stepwise changes in carboxyhemoglobin.

Figure 4. The plot of absorbance of 940 nm/ absorbance at 805 nm versus the percentage of oxyhemoglobin. The narrow separation between varying carboxyhemoglobin levels indicates difficulty in separating out carboxyhemoglobin at this set of wavelengths.

Figure 5. The overlay of Fig. 2 and Fig. 3. The horizontal lines indicate all the possible solutions to the equations. The vertical line gives the unique solution where HbO_2 is common for both.

Figure 6. The emitter board consists of three custom mounted LED dies wire bonded and mounted on gold inlay.

Figure 7. The circuit diagram inside the sensor shows

the three LED dies transmitting to a photovoltaic cell and amplifier which amplifies and filters the output.

Figure 8. Block diagram of the three-wavelength oximeter.

Figure 9. Flowchart for general control and signal processing of the oximeter.

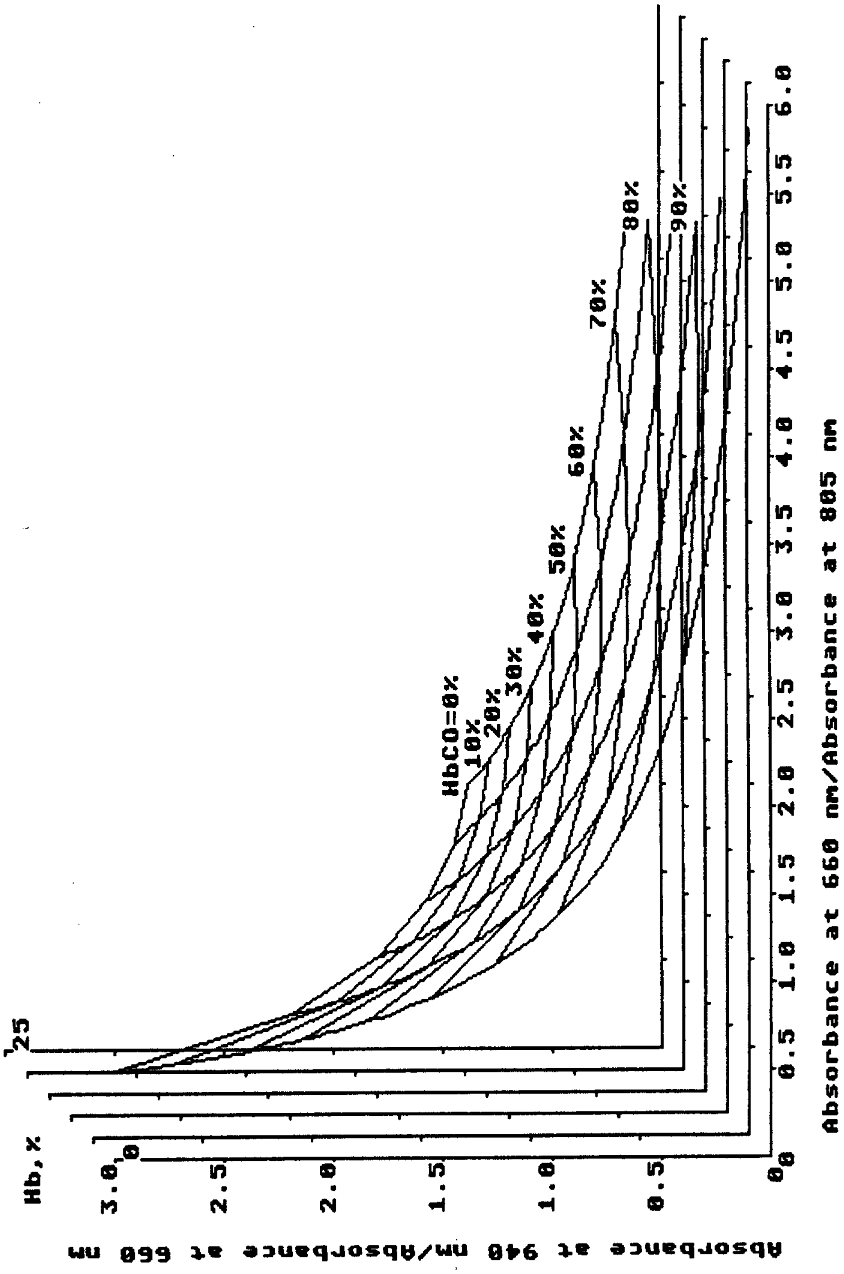
Absorbance at 940 nm/Absorbance at 660 nm
Absorbance at 660 nm/Absorbance at 805 nm
Hb, %
0
25
3.0
2.5
2.0
1.5
1.0
0.5
0
0.5
1.0
1.5
2.0
2.5
3.0
3.5
4.0
4.5
5.0
5.5
6.0
HbCO=0%
10%
20%
30%
40%
50%
60%
70%
80%
90%

FIGURE 1

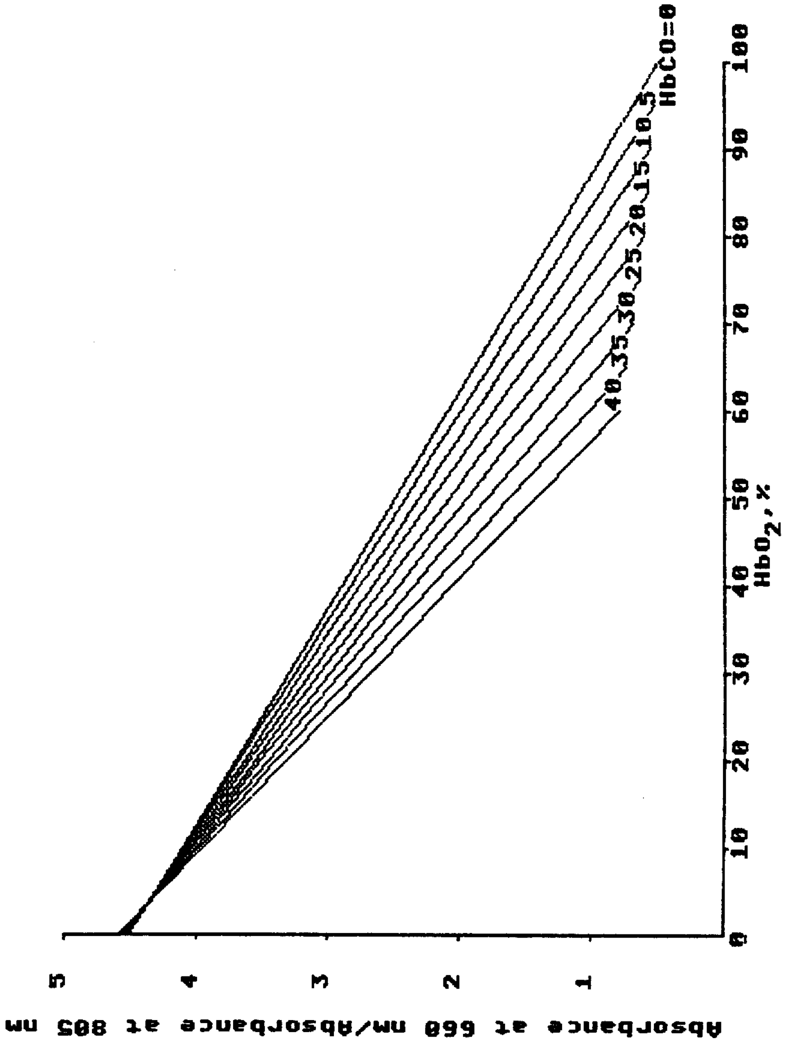
Absorbance at 660 nm/Absorbance at 805 nm
1
2
3
4
5
0
10
20
30
40
50
60
70
80
90
100
HbO$_2$,%
HbCO=0
5
10
15
20
25
30
35
40

FIGURE 2

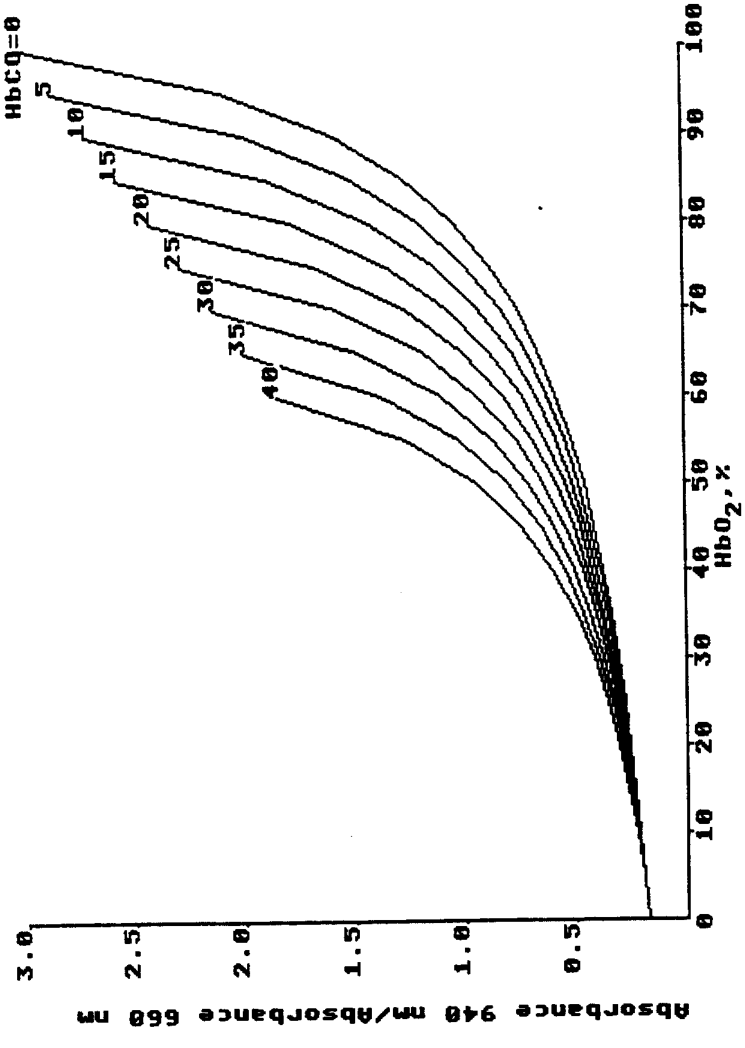
HbCO=0
5
10
15
20
25
30
35
40
3.0
2.5
2.0
1.5
1.0
0.5
Absorbance 940 nm/Absorbance 660 nm
0
10
20
30
40
50
60
70
80
90
100
HbO2, %

FIGURE 3

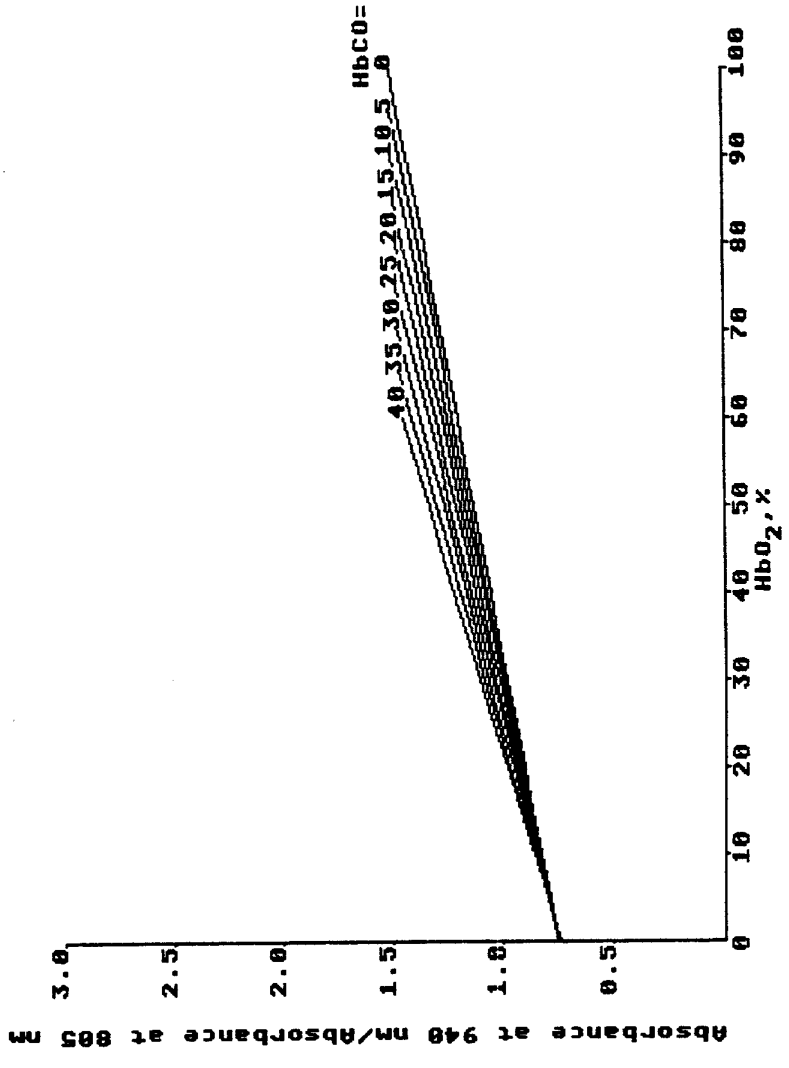
HbCO=
0
5
10
15
20
25
30
35
40
Absorbance at 940 nm/Absorbance at 805 nm
3.0
2.5
2.0
1.5
1.0
0.5
0
10
20
30
40
50
60
70
80
90
100
HbO2,%

FIGURE 4

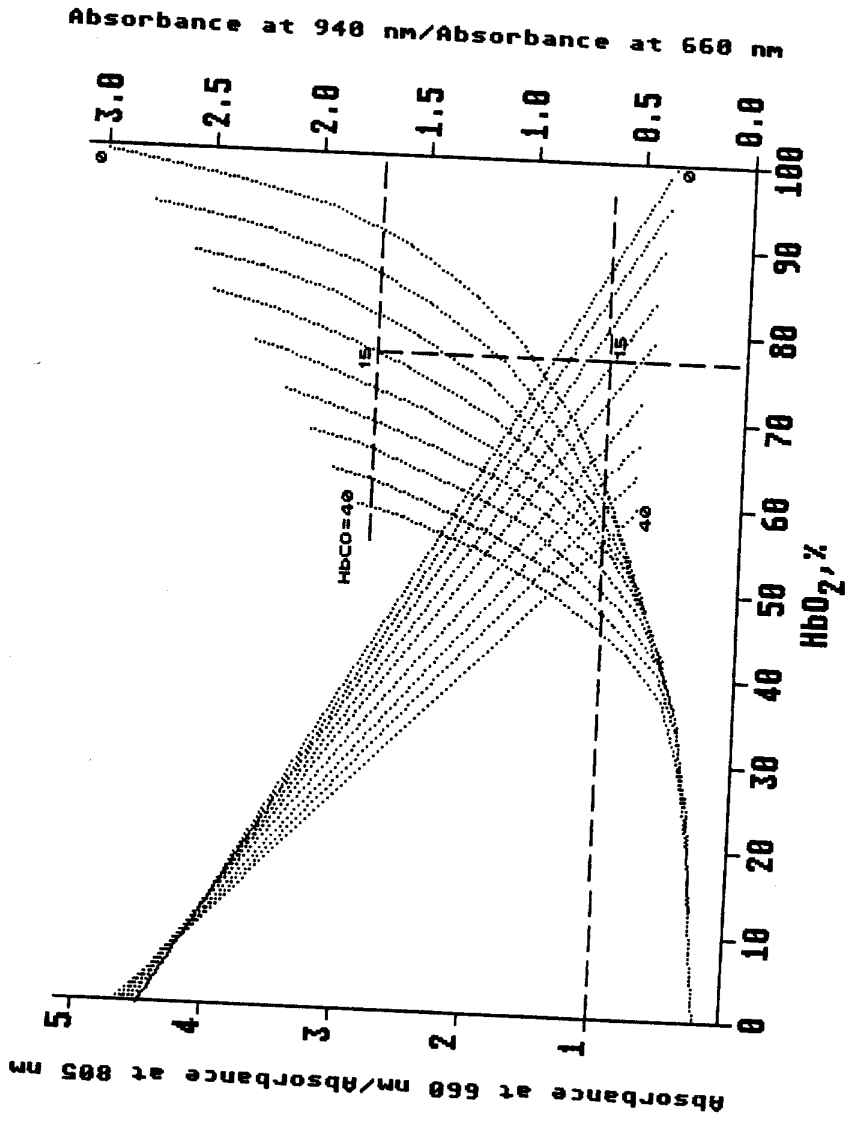
Absorbance at 940 nm/Absorbance at 660 nm
3.0
2.5
2.0
1.5
1.0
0.5
0.0
HbO$_2$,%
0
10
20
30
40
50
60
70
80
90
100
Absorbance at 660 nm/Absorbance at 805 nm
5
4
3
2
1
0
HbCO=40
15
15
40
0
0

FIGURE 5

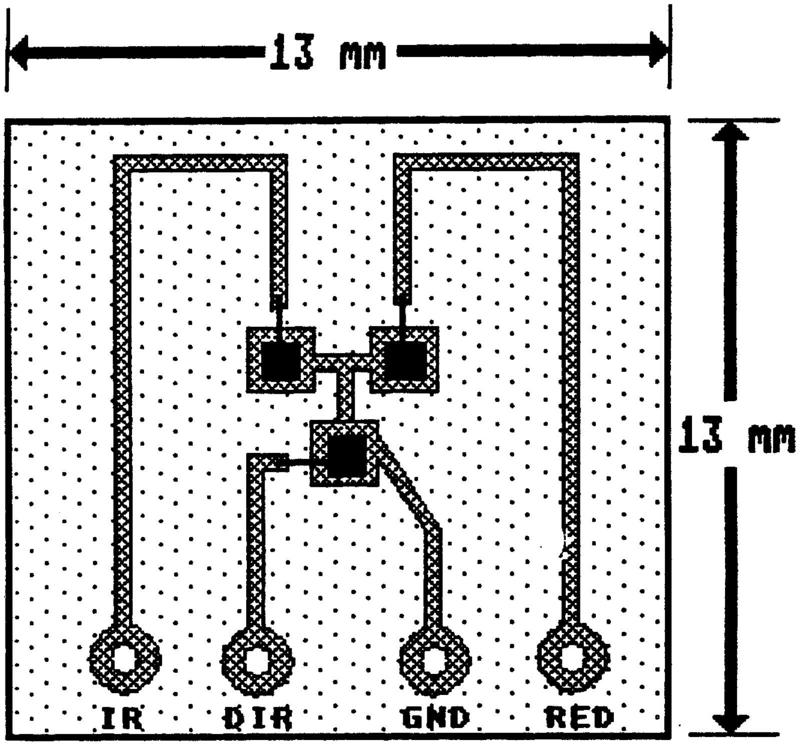

FIGURE 6

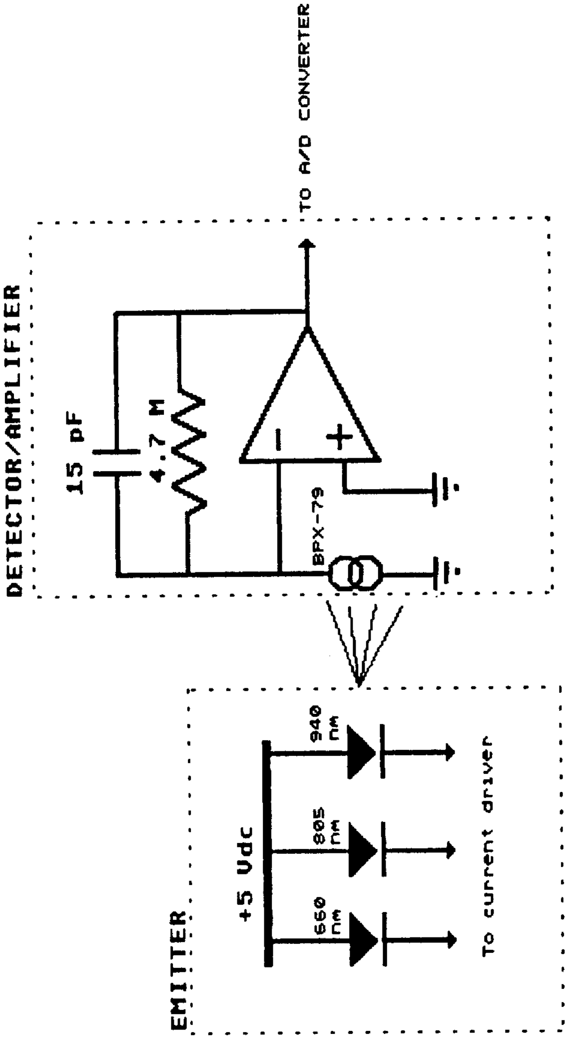
DETECTOR/AMPLIFIER
15 pF
4.7 M
BPX-79
TO A/D CONVERTER
EMITTER
+5 Vdc
660 nm
805 nm
940 nm
To current driver

FIGURE 7

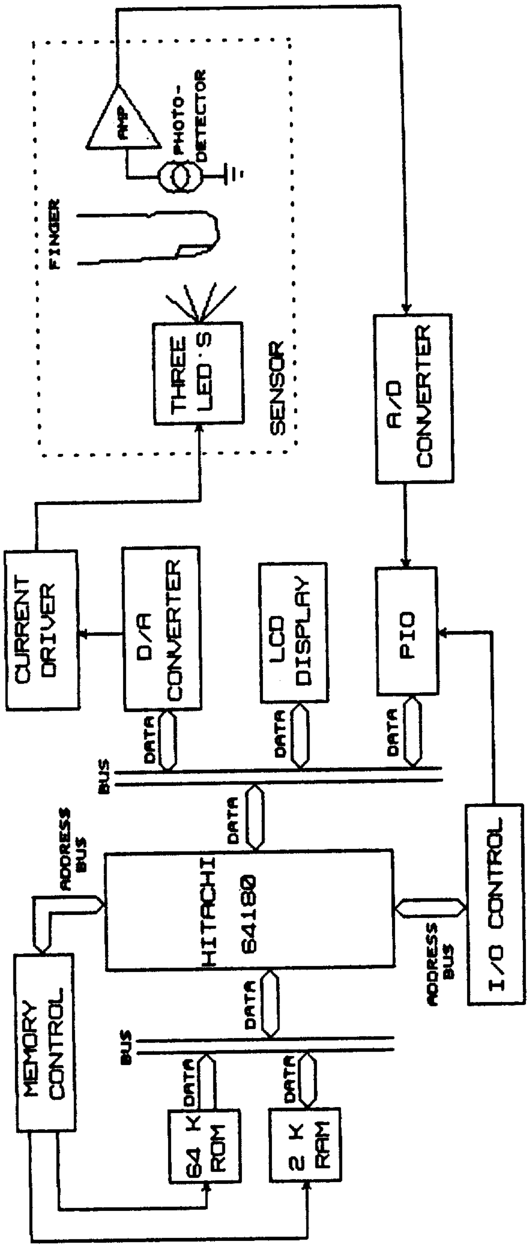
SENSOR
THREE LED'S
FINGER
AMP
PHOTO-DETECTOR
A/D CONVERTER
CURRENT DRIVER
D/A CONVERTER
LCD DISPLAY
PIO
DATA
DATA
DATA
BUS
DATA
ADDRESS BUS
HITACHI 64180
ADDRESS BUS
I/O CONTROL
MEMORY CONTROL
DATA
BUS
DATA
DATA
64 K ROM
2 K RAM

FIGURE 8

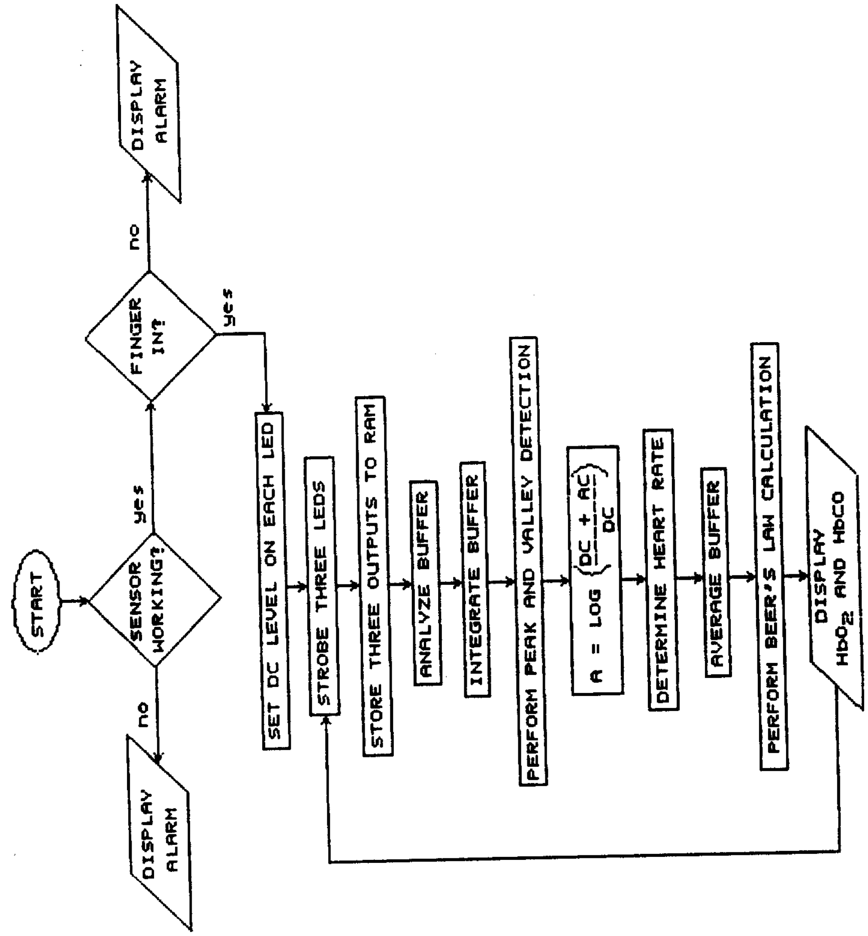
START
SENSOR WORKING?
no
DISPLAY ALARM
yes
FINGER IN?
no
DISPLAY ALARM
yes
SET DC LEVEL ON EACH LED
STROBE THREE LEDS
STORE THREE OUTPUTS TO RAM
ANALYZE BUFFER
INTEGRATE BUFFER
PERFORM PEAK AND VALLEY DETECTION
$A = \text{LOG}\left\{\frac{DC + AC}{DC}\right\}$
DETERMINE HEART RATE
AVERAGE BUFFER
PERFORM BEER'S LAW CALCULATION
DISPLAY HbO_2 AND HbCO

FIGURE 9

Approved

John G. Webster

May 14, 1987